

# Clinical characteristics and biomarkers of breast cancer associated with choline concentration measured by $^1\text{H}$ MRS

J.-H. Chen<sup>a,b\*,†</sup>, R.S. Mehta<sup>c,†</sup>, H.-M. Baek<sup>a</sup>, K. Nie<sup>a</sup>, H. Liu<sup>a</sup>, M.Q. Lin<sup>a</sup>, H.J. Yu<sup>a</sup>, O. Nalcioglu<sup>a</sup> and M.-Y. Su<sup>a</sup>

This study investigated the association between the total choline (tCho) concentration and the clinical characteristics and biomarker status of breast cancer. Sixty-two patients with breast cancer, 1.5 cm or larger in size on MR images, were studied. The tCho concentration was correlated with the MRI features, contrast enhancement kinetics, clinical variables and biomarkers. Pairwise two-tailed Spearman's nonparametric test was used for statistical analysis. The tCho concentration was higher in high-grade than moderate-/low-grade tumors ( $p = 0.04$ ) and in tumors with higher  $K_{\text{trans}}$  and  $k_{\text{ep}}$  ( $p < 0.001$  for both). The association of tCho concentration with age ( $p = 0.05$ ) and triple negative biomarker ( $p = 0.09$ ) approached significance. tCho was not detected in 17 patients, including 15 with invasive ductal cancer and two with infiltrating lobular cancer. Fifteen of the 17 patients had moderate- to low-grade cancers, and 11 had human epidermal growth factor-2-negative cancer, suggesting that these two factors might lead to false-negative choline. Higher tCho concentration in high-grade tumors and tumors with higher  $K_{\text{trans}}$  and  $k_{\text{ep}}$  indicates that choline is associated with cell proliferation and tumor angiogenesis. The higher choline level in younger women may be caused by their more aggressive tumor type. The results presented here may aid in the better interpretation of  $^1\text{H}$  MRS for the diagnosis of breast lesions. Copyright © 2010 John Wiley & Sons, Ltd.

**Keywords:** biomarkers; breast cancer; choline concentration;  $^1\text{H}$  MRS

## INTRODUCTION

Choline-containing compounds are the major components of the cell membrane required for structural stability and cell proliferation (1). Many studies have shown that the total choline (tCho) peak is elevated in neoplastic tissues. The increased tCho concentration in neoplastic tissues may be a result of increased membrane turnover by replicating cells. However, the precise mechanisms that produce an elevated tCho concentration are not yet fully understood. The level of tCho may vary as a result of numerous changes in enzymatic activity and fluxes in biosynthetic and catabolic pathways in which choline compounds serve as both precursors and catabolites (2). The choline signal can be measured using *in vivo*  $^1\text{H}$  MRS. The choline peak is found in the MR spectra resonating at 3.2 ppm, with the main contribution from phosphocholine (3).

$^1\text{H}$  MRS has become an adjunct to dynamic contrast-enhanced MRI (DCE-MRI) in the clinical evaluation of breast lesions. Malignant lesions are more likely than benign or normal breast tissues to show high levels of choline-containing compounds, and this observation may serve as the basis for differentiating between malignant and benign breast lesions. Previous studies performed using 1.5-T MR have reported sensitivities of 70–100% (average, 89%) and specificities of 67–100% (average, 87%) for breast MRS (4–11). Katz-Brull *et al.* (12) analyzed five studies and reported an overall sensitivity of 83% and specificity of 85%. Despite the promising results demonstrated in these studies,

$^1\text{H}$  MRS has a false-negative rate of approximately 4–18% and a false-positive rate of 14–18% (4–6,13), and can only be used to provide additional information for the characterization of detected lesions.

The underlying mechanisms for the elevated level of choline-containing compounds in breast cancer have been investigated extensively. As the choline level represents a proliferative marker,

\* Correspondence to: J.-H. Chen, Center for Functional Onco-Imaging, School of Medicine, University of California Irvine, 164 Irvine Hall, Irvine, CA 92697, USA.

a J.-H. Chen, H.-M. Baek, K. Nie, H. Liu, M.Q. Lin, H.J. Yu, O. Nalcioglu, M.-Y. Su Tu & Yuen Center for Functional Onco-Imaging, University of California, Irvine, CA, USA

b J.-H. Chen  
Department of Radiology, China Medical University Hospital, Taichung, Taiwan

c R. Mehta  
Department of Medicine, University of California, Irvine, CA, USA

† These authors contributed equally to this work.

**Abbreviations used:** ACR BI-RADS, American College of Radiology Breast Imaging Reporting and Data System; DCE, dynamic contrast-enhanced; DCIS, ductal carcinoma in situ; ER, estrogen receptor; HER-2, human epidermal growth factor-2; IDC, invasive ductal carcinoma; ILC, infiltrating lobular cancer;  $k_{\text{ep}}$ , washout rate;  $K_{\text{trans}}$ , uptake rate; PR, progesterone receptor; tCho, total choline; TN, triple negative.

many biological factors may affect its concentration within the tumor. It would be of interest to evaluate the biological parameters of benign and malignant lesions that might affect the outcome of <sup>1</sup>H MRS. It has been reported that the degree of elevated choline-containing compounds is related to the grade of the tumor, with higher levels in high-grade than in low-grade lesions (14,15). The relationship between the presence of choline-containing compounds and other commonly analyzed breast cancer biomarkers, such as estrogen receptor (ER), progesterone receptor (PR) and HER-2 receptor, has been studied less extensively (16–18).

The false-negative results in breast cancer based on tCho concentration measured by <sup>1</sup>H MRS may be related in part to other characteristic parameters. The purpose of this study was to conduct a systematic analysis of the relationship between the choline concentration measured by <sup>1</sup>H MRS and the known diagnostic and prognostic markers of breast cancer, including the clinical characteristics, tumor phenotype and biomarker status of breast cancer.

## MATERIALS AND METHODS

### Patients

Subjects were identified from a retrospective review of our research breast MRI database of all patients who received a scan protocol, including DCE-MRI and a single-voxel <sup>1</sup>H MRS sequence, between 2003 and 2006. The inclusion criteria were patients with a biopsy-confirmed diagnosis of malignant lesions measuring

1.5 cm or larger on MR images. The <sup>1</sup>H MRS voxel size used in this study was 1.5–2.0 cm in one dimension. If fibroglandular tissues are contained in the MRS voxel, this will lead to a lower choline concentration; if fatty tissues are contained in the MRS voxel, this may further degrade the spectral quality. Therefore, lesions smaller than 1.5 cm were excluded to minimize the impact of the partial volume effect.

Sixty-two patients were identified. Table 1 summarizes the number of patients in each category: tumor type [invasive ductal carcinoma (IDC) or infiltrating lobular cancer (ILC)], tumor grade (I, II, III), tumor morphology (mass or nonmass), HER-2 (positive or negative), ER (positive or negative), PR (positive or negative), hormonal receptor (positive or negative) and triple negative (TN) (yes or no). All 62 subjects received pre-therapy <sup>1</sup>H MRS. Either surgery (*n* = 29) or neoadjuvant chemotherapy (*n* = 33) was performed after the MRI/MRS study. The patient age ranged from 31 to 78 years, with a mean age of 54 years. The clinical variables and biomarkers, including patient age, tumor histologic type, tumor grade, ER, PR and HER-2, were analyzed. The association between choline and lesion features appearing on MRI, including mass lesions vs nonmass-like enhancements and the contrast enhancement pharmacokinetic parameters, was also analyzed. This study was approved by the institutional review board and all participants gave written informed consent.

### MRI protocol

The MRI study was performed using a 1.5-T Phillips Eclipse MR scanner with a standard bilateral breast coil (Philips Medical

**Table 1.** Clinical and imaging characteristics of the 62 women

	Number of cases	%
Tumor type ( <i>n</i> = 62)		
Invasive ductal carcinoma	55	89
Infiltrating lobular cancer	7	11
Tumor grade ( <i>n</i> = 57, 5 unknown)		
I	9	16
II	28	49
III	20	35
Tumor morphology ( <i>n</i> = 62)		
Mass	43	69
Nonmass	19	31
Human epidermal growth factor-2 ( <i>n</i> = 55, 7 unknown)		
Positive	18	34
Negative	37	66
Estrogen receptor ( <i>n</i> = 54, 8 unknown)		
Positive	34	63
Negative	20	37
Progesterone receptor ( <i>n</i> = 47, 15 unknown)		
Positive	26	55
Negative	21	45
Hormonal receptor ( <i>n</i> = 54, 8 unknown)		
Positive	35	65
Negative	19	35
Triple negative tumor ( <i>n</i> = 56)		
Yes	11	20
No	45	80

\*\*For the number of patients the status was unknown means that for these patients there were no results available.

Systems, Cleveland, OH, USA). The imaging protocol consisted of high-resolution pre-contrast  $T_1$ -weighted imaging, bilateral DCE-MRI and MRS. After the localizer scan to define the location of the breasts, sagittal view unilateral pre-contrast  $T_1$ -weighted images were acquired using a spin-echo pulse sequence. A three-dimensional, spoiled gradient-recalled echo, radiofrequency Fourier-acquired steady-state pulse sequence with 16 frames (repetitions) was then utilized for bilateral dynamic imaging. A total of 32 axial slices with a thickness of 4 mm was used to acquire dynamic data from both breasts. The following imaging parameters were used: TR = 8.1 ms; TE = 4.0 ms; flip angle, 20°; matrix size, 256 × 128; field of view, 30–35 cm. The scan time was 42 s per acquisition. The sequence was repeated 16 times for dynamic acquisitions, including four pre-contrast sets and 12 post-contrast sets. The contrast agent (Omniscan, 0.1 mmol/kg) was manually injected at the beginning of the fifth acquisition, and was timed to finish in 12 s in order to standardize the bolus length for all patients. Immediately following the contrast, 10 cm<sup>3</sup> of saline were injected to flush in all contrast medium.

### <sup>1</sup>H MRS protocol and analysis

After completing DCE-MRI, the acquisition of the MR spectrum was performed using the localized single-voxel technique with the point-resolved spectroscopic sequence (19). The spectroscopic voxel was placed by a spectroscopist (HMB) on the subtraction images at 1 min post-injection generated on the scanner console (using DCE frame #6–frame #3). The voxel size was from 3.4 cm<sup>3</sup> (1.5 × 1.5 × 1.5 cm<sup>3</sup>) to 8.0 cm<sup>3</sup> (2 × 2 × 2 cm<sup>3</sup>). It was carefully positioned to maximize coverage of the enhanced lesion on the subtraction images, and to minimize the inclusion of adipose tissue on pre-contrast nonfat-saturated images. Voxel shimming was performed for the optimization of field homogeneity, and the typical linewidth of the water peak (full width at half-maximum) was 8–17 Hz. Water suppression was performed using three-pulse chemical shift-selective RF pulses (20), and the fat signal was independently attenuated using a frequency-selective lipid suppression technique. The point-resolved spectroscopic sequence parameters were as follows: TE = 270 ms; ms; TR = 2000 ms; data points, 2048; spectral bandwidth, 1953 Hz; acquisition averages, 128. A fully relaxed, unsuppressed spectrum (24 averages) was also acquired to measure the water and lipid peaks as the internal reference for calculating the absolute choline concentration (mmol/kg) (21,22). The absolute tCho levels were quantified using a Gaussian lineshape fitting model, and the unsuppressed water signal was used as an internal reference (22).

### Analysis of enhancement time course

The enhancement kinetics of the lesion were measured from a hotspot region of interest. A computer algorithm was used to search an area of 3 × 3 pixels on one image slice within the whole tumor that showed the strongest enhancement on subtraction images at 2 min post-injection as the hotspot region of interest. The maximum intensity projection was used as reference. The percentage enhancement time course was calculated by subtracting the pre-contrast signal intensity (mean of first four frames) from each of the subsequent 12 post-contrast signal intensities, and then normalized to the pre-contrast signal intensity to calculate the enhancement percentage. The enhancement kinetics were further

analyzed on the basis of the two-compartmental pharmacokinetic model described by Tofts *et al.* (23,24) to obtain the transfer constant  $K_{trans}$  and rate constant  $k_{ep}$  (representing the uptake rate and washout rate, respectively).

### Interpretation of MRI features based on the American College of Radiology Breast Imaging Reporting and Data System (ACR BI-RADS) lexicon

The presentation of the lesion on MR images was analyzed by a radiologist (JHC) with extensive experience in body imaging and breast MRI. Morphological and enhancement kinetic features were evaluated in concordance with the ACR BI-RADS lexicon (25). Morphological diagnosis included mass type with well-defined tumor boundaries (including foci of < 5 mm and a mass ≥ 5 mm) and nonmass-like enhancement lesions that enhance in an area that is neither a mass nor a blood vessel. Tumor size was measured on the basis of the longest dimension and the longest perpendicular dimension shown on maximum intensity projection.

### Analysis of tumor grade and biomarkers

The tumor grade and biomarker status were examined by pathologists at our institution using the standard clinical protocol. The modified Bloom and Richardson tumor grades I, II and III (indicating low, moderate and high grade) were used in the analysis. The ER and PR status was considered to be negative if immunoperoxidase staining of tumor cell nuclei in the biopsy specimen was less than 5%. The expression of HER-2 protein in the tumor was measured using immunohistochemical analysis on a scale from 0 to 3+. A score of 3+ on immunohistochemistry indicates positive HER-2; and scores of 0 to 1+ indicate negative HER-2. Patients with a score of 2+ were further examined using fluorescence *in situ* hybridization. A tumor is designated as 'positive' for Her-2 gene amplification if the gene-to-chromosome ratio is > 2.0. When ER or PR is positive, the cancer is hormonal receptor positive, and when ER, PR and HER-2 are all negative, the cancer is TN.

### Statistics

The association between all considered variables, including tCho concentration, clinical characteristics, tumor phenotypes and biomarker status, was evaluated. Age and choline concentration were continuous variables. The enhancement kinetic parameters  $K_{trans}$  and  $k_{ep}$  were also continuous variables. The tumor type was separated as IDC or ILC. The tumor grade was categorized as I (low), II (moderate) and III (high). The tumor morphology was separated into mass lesions or nonmass lesions. The biomarkers, including ER, PR, HER-2, hormonal receptor and TN, were categorized as positive or negative. The pairwise association was analyzed using a two-tailed Spearman's nonparametric test with pairwise deletion of missing data. For nonparametric correlation, all data were treated based on their own rank in the whole dataset. This does not require numerical values or any assumption about the distribution. However, parametric correlation (Pearson's correlation) can be used for the comparison of numerical values, and requires that the dataset should be normally distributed.

The correlation coefficient  $r$  was used to quantify the correlation value about two variables, and the  $p$  value measures the probability of independence of the two variables. If the absolute  $r$  value is in the range of (0, 0.3), it indicates that the two variables are poorly correlated. If the absolute  $r$  value is in the range of (0.3, 0.5), it

indicates that the two variables are moderately correlated. If the absolute  $r$  value is in the range of (0.5, 1), it indicates that the two variables are highly correlated. For  $p$ , if  $p < 0.05$ , the two variables are correlated. If  $p > 0.05$ , the two variables are not correlated.

To interpret the study results, we first checked the  $p$  value to determine whether the two variables were correlated ( $p < 0.05$ ) or not ( $p \geq 0.05$ ). Then, we checked the correlation coefficient  $r$  to see how much they were correlated ( $r < 0.3$ , poor correlation;  $0.3 < r < 0.5$ , moderate correlation;  $r > 0.5$ , high correlation). When  $p$  was small ( $p < 0.05$ ) and  $r$  was small (absolute  $r < 0.3$ ), the data sample was diversely distributed (distribution and/or small sample size).

## RESULTS

The results of the pairwise association among all the analyzed variables are shown in Table 2. ER and PR were highly correlated ( $r = 0.87$ ,  $p < 0.001$ ), which was the strongest correlation among all analyses, a well-known fact. Patients with IDC were more likely to present mass lesions ( $r = -0.43$ ,  $p < 0.001$ ). Younger patients were more likely to have higher choline ( $p = 0.05$ ) and to present TN cancer ( $r = 0.32$ ,  $p = 0.02$ ). HER-2-positive cancer was more likely to be of high grade ( $r = 0.36$ ,  $p = 0.01$ ).

The measured tCho level showed a wide range, 0.08–9.99 ( $1.9 \pm 2.3$  mmol/kg), but the high variation was consistent with the previously published value of 1.38–10 mmol/kg by Bolan *et al.* (21). Higher tCho concentration showed a significant correlation with higher tumor grade ( $r = 0.38$ ,  $p = 0.04$ ) (Figs. 1 and 2). The association of tCho with age and TN status approached significance ( $p = 0.05$  and  $p = 0.09$ , respectively) (Fig. 3). Analysis of DCE pharmacokinetic parameters found that a higher  $K_{trans}$  was associated with a younger age ( $r = -0.3$ ,  $p = 0.02$ ) and a higher tumor grade ( $r = 0.32$ ,  $p = 0.02$ ); higher  $K_{trans}$  and  $k_{ep}$  were associated with a higher choline level ( $r = 0.54$ ,  $p < 0.001$ ;  $r = 0.53$ ,  $p < 0.001$ ) and TN tumor ( $r = -0.36$ ,  $p = 0.01$ ;  $r = -0.36$ ,  $p = 0.01$ ). The results of tCho,  $K_{trans}$  and  $k_{ep}$  in different tumor types, tumor grades, MR phenotypes and biomarkers status are listed in Table 3.

Seventeen patients showed false-negative results of tCho in our study, including 15 with IDC and two with ILC. Eleven patients were HER-2 negative (Fig. 4), four patients were HER-2 positive (Figs. 5 and 6) and the other two patients' HER-2 results were not available. Of these 17 patients, 15 had moderate- to low-grade cancers and two had high-grade tumor (Fig. 4), four had extensive ductal carcinoma *in situ* (DCIS) and five had nonmass-like enhancement lesions. The results suggested that negative HER-2 (when in combination with positive ER) and low tumor grade were two likely factors leading to false-negative choline.

**Table 2.** Correlation of age, MRI features and clinical characteristics

	MRI features						Clinical characteristics			
	tCho level	Tumor type	Tumor grade	Morphology	$K_{trans}$	$k_{ep}$	Her-2	ER	PR	TN
Age	- 0.25 (0.05)	0.26 (0.04 <sup>a</sup> )	- 0.26 (0.04 <sup>a</sup> )	0.01 (0.94)	- 0.30 (0.02 <sup>a</sup> )	- 0.29 (0.02 <sup>a</sup> )	- 0.07 (0.62)	0.23 (0.09)	0.14 (0.36)	0.32 (0.02 <sup>a</sup> )
tCho level		0.03 (0.84)	0.38 (0.04 <sup>a</sup> )	0.03 (0.79)	0.54 ( $< 0.001^a$ )	0.53 ( $< 0.001^a$ )	- 0.03 (0.85)	- 0.11 (0.41)	0.08 (0.56)	- 0.23 (0.09)
Tumor type			- 0.28 (0.03 <sup>a</sup> )	- 0.43 ( $< 0.001^a$ )	- 0.19 (0.13)	- 0.24 (0.06)	- 0.22 (0.10)	0.24 (0.08)	0.27 (0.07)	0.15 (0.26)
Tumor grade				0.24 (0.07)	0.32 (0.02 <sup>a</sup> )	0.29 (0.03 <sup>a</sup> )	0.36 (0.01 <sup>a</sup> )	- 0.27 (0.04 <sup>a</sup> )	- 0.22 (0.13)	- 0.22 (0.11)
Morphology					0.10 (0.45)	0.17 (0.18)	0.09 (0.50)	- 0.04 (0.78)	- 0.02 (0.87)	- 0.009 (0.95)
$K_{trans}$						0.95 ( $< 0.001^a$ )	- 0.02 (0.89)	- 0.25 (0.07)	- 0.24 (0.11)	- 0.36 (0.01 <sup>a</sup> )
$k_{ep}$							0.06 (0.67)	- 0.28 (0.04 <sup>a</sup> )	- 0.29 (0.04 <sup>a</sup> )	- 0.36 (0.01 <sup>a</sup> )
Her-2								- 0.14 (0.31)	- 0.17 (0.26)	0.35 (0.007 <sup>a</sup> )
ER									0.87 ( $< 0.001^a$ )	0.66 ( $< 0.001^a$ )
PR										0.62 ( $< 0.001$ )

ER, estrogen receptor; HER-2, human epidermal growth factor-2;  $k_{ep}$ , washout rate;  $K_{trans}$ , uptake rate; PR, progesterone receptor; tCho, total choline; TN, triple negative.

The data format presented in the table is: correlation coefficient  $r$  and ( $p$  value).

Age, tCho,  $K_{trans}$  and  $k_{ep}$  are continuous variables; morphology, tumor type, ER, PR, HER-2 and TN are dichotomized variables; the tumor grade is a categorized variable (I–III).

<sup>a</sup>Denotes statistically significant correlation ( $p = 0.05$ ) of the two variables.

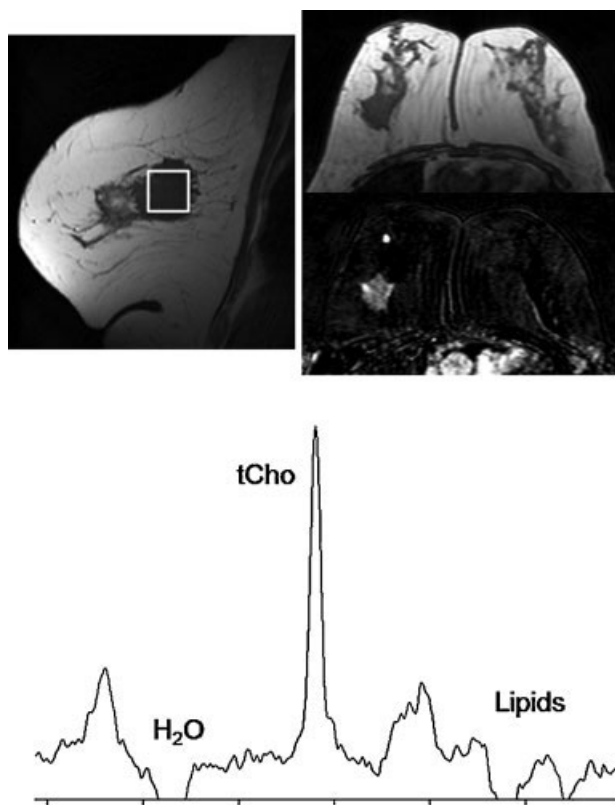


**Figure 1.** A 62-year-old woman with a 3.4 × 3.3-cm, high-grade, invasive ductal cancer in the right breast. <sup>1</sup>H MRS showed a high choline peak (6.97 mmol/kg) at 3.2 ppm. Biomarker information was not available in this patient.

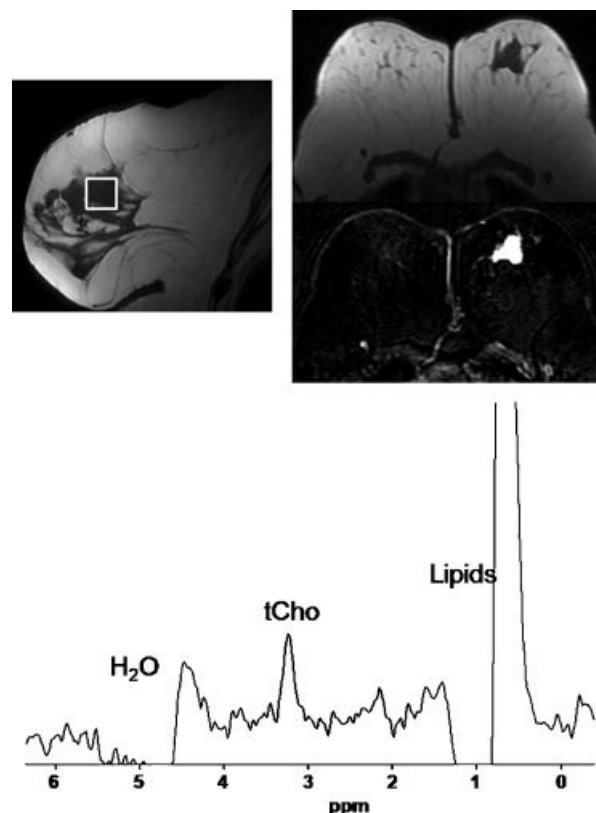


**Figure 2.** A 66-year-old woman with a 2.7 × 2.6-cm, moderate-grade, human epidermal growth factor-2-negative, estrogen receptor-positive, invasive ductal cancer in the left breast. <sup>1</sup>H MRS showed a low choline peak (1.79 mmol/kg) at 3.2 ppm.

## DISCUSSION

The addition of single-voxel <sup>1</sup>H MRS could improve the diagnostic specificity of DCE-MRI (9,22). Bartella *et al.* (11) found that the use of <sup>1</sup>H MRS increased significantly the positive predictive value of biopsy from 35% to 82% and obviated biopsy in 57% of the 40 lesions with unknown histologic features. Huang *et al.* (10) also showed that the addition of <sup>1</sup>H MRS to a conventional MRI protocol increased the specificity from 62.5% to 87.5%.

Although <sup>1</sup>H MRS has shown promising results for the evaluation of breast cancer, a number of false-negative findings in various *in situ* and invasive lesions have been reported (4,5,7). The failure to detect choline in some breast cancers might be related to insufficient sensitivity, such as for small or less aggressive tumors. Other problems, including patient motion, contamination by hemorrhage (5), the inclusion of fatty tissue (6) and tumor cells growing with many intervening stromal cells and inflammatory cells (26), could also lead to false-negative results. In studies to characterize the dependence of breast <sup>1</sup>H MRS sensitivity on lesion size, the sensitivity in three different size groups (< 2.5, 2.5–4.9 and ≥ 5 cm) increased from 72% to 90% to 100% (5–7). In this study, we only selected patients with a tumor size larger than 1.5 cm. In small lesions, the MRS voxel size may be larger than the tumor size. If fibroglandular tissues are contained within the MRS voxel, this will lead to a lower choline; if fatty tissues are contained in the MRS voxel, this may further degrade the spectral quality. Therefore, in either scenario, the spectrum suffers from the contamination of normal tissues, and does not reflect the true characteristics of the cancerous tissues. Many biological factors

likely to affect the measurement of choline by <sup>1</sup>H MRS need to be investigated to understand the intrinsic limitation of <sup>1</sup>H MRS for the characterization of breast lesions.

In our study, higher tCho levels were correlated with higher  $K_{trans}$  and  $k_{ep}$  ( $p < 0.001$  for both). However, it should be noted that the hotspot size was 3 × 3 pixels on one slice (4 mm), with a total of nine pixels. The MRS voxel was much larger than the DCE hotspot. Therefore, these datasets are not meant for spatial correlation, but rather for the characterization of different properties of the tumor (that is, vascular and metabolic) for the investigation of their associations. We have published two other studies (27,28) comparing the DCE and MRS results analyzed from spatially coregistered tissues. Su *et al.* (27) reported a study correlating the pharmacokinetic parameters in DCE-MRI with choline measured by <sup>1</sup>H MRS using a chemical shift imaging method in 14 patients. It was shown that, by averaging over all choline-positive voxels, there was a significant linear correlation between choline and percentage enhancement at 2 min after injection ( $r = 0.75$ ,  $p = 0.002$ ) and the pharmacokinetic parameters  $K_{trans}$  ( $r = 0.74$ ,  $p = 0.003$ ) and  $k_{ep}$  ( $r = 0.76$ ,  $p = 0.002$ ). Baek *et al.* (28) studied 32 patients using single-voxel <sup>1</sup>H MRS and found a significant correlation between tCho and the pharmacokinetic parameter  $k_{ep}$  ( $r = 0.62$ ,  $p < 0.0001$ ), indicating that tissues with a high choline level have higher washout rates in DCE MRI. A subcohort of 20 subjects reported in that study was analyzed in this work. The results suggested that, overall, there is a correlation between choline metabolism and angiogenesis activity. The finding that higher  $K_{trans}$  and  $k_{ep}$  are significantly associated with a younger

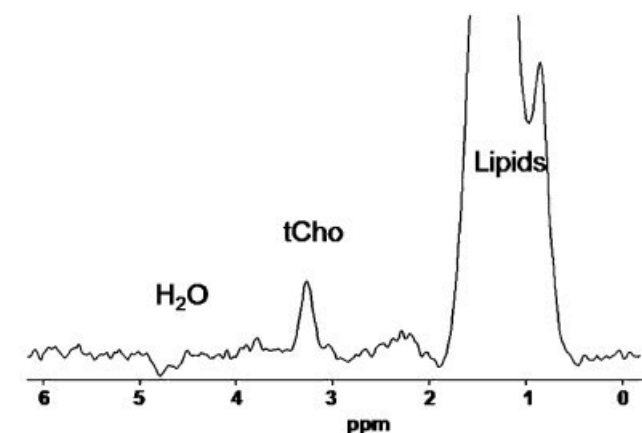
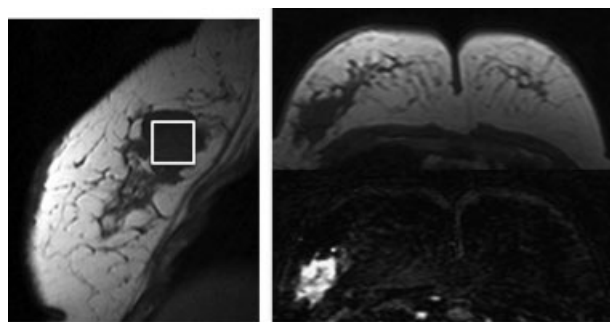


**Figure 3.** A 35-year-old woman with a 3.5 × 2.7-cm, high-grade, triple negative, invasive ductal cancer in the right breast. <sup>1</sup>H MRS showed a choline peak (4.33 mmol/kg) at 3.2 ppm.

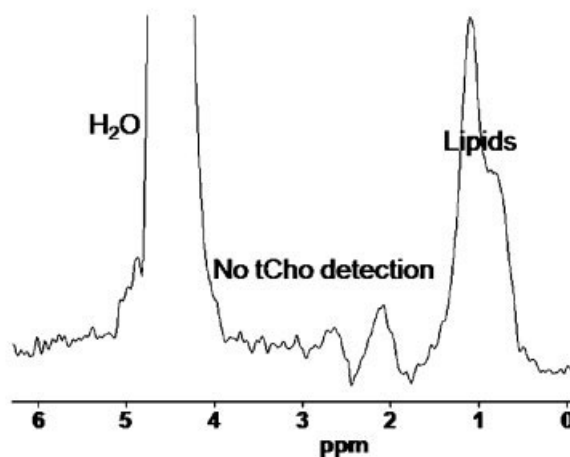
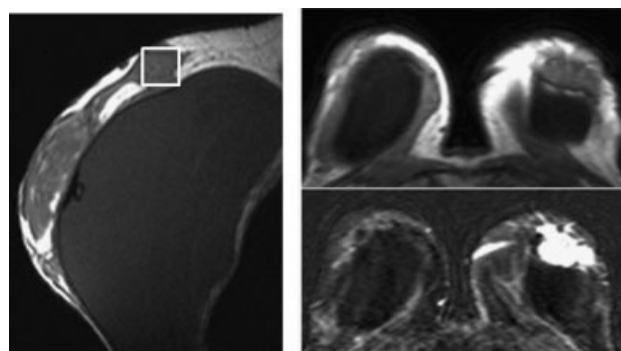


**Figure 4.** A 32-year-old woman, status post-breast augmentation, with a 3.5 × 2.0-cm, ill-defined margin, heterogeneously enhanced, invasive ductal cancer in the left breast. The tumor was high grade, human epidermal growth factor-2 negative and hormonal positive. The choline peak was not detectable in <sup>1</sup>H MRS.

age and TN cancer suggests that angiogenesis is greater in more aggressive breast cancer.

Lesions with a higher tCho level were more likely to show a higher tumor grade ( $p = 0.04$ ). Smith *et al.* (15) measured the content of choline-related metabolites in chemical extracts of 46 human breast carcinomas using <sup>31</sup>P NMR spectroscopy, and found that the phosphocholine content was higher in high-grade tumors when compared with low-grade tumors. In our study, high-grade breast cancer was more likely in ER-negative tumors ( $p = 0.04$ ). Negative ER in breast cancer is considered to be a poor prognostic indicator. Compared with their ER-positive counterparts, the cells are more likely to be poorly differentiated and more aggressive. ER-negative tumors were characterized by a higher proliferative activity, and a significant association between choline kinase overexpression and high histologic tumor grade

and ER-negative status has been reported (29). This association is possibly mediated through higher cell proliferation (5).

Although HER-2-positive cancer was more likely to be of high tumor grade ( $p = 0.01$ ), tCho did not show a significant difference between HER-2-positive and HER-2-negative cancer. In our study, <sup>1</sup>H MRS showed 17 false-negative diagnoses. Of these, 15 were moderate- or low-grade tumors and 11 were HER-2-negative cancers. It was therefore suggested that HER-2-negative cancer of moderate or low grade was more likely to be tCho negative (9). HER-2 receptor mediates signaling to cancer cells and stimulates proliferation (30,31). HER-2/neu is overexpressed in 20–25% of invasive breast cancers and associated with an aggressive tumor,

**Table 3.** Measurements of total choline (tCho), uptake rate ( $K_{trans}$ ) and washout rate ( $k_{ep}$ ) in different tumor types, tumor grades, MR phenotypes and biomarker status

	Tumor type		Tumor grade			Morphology		HER-2		ER		PR		TN	
	IDC	ILC	I	II	III	Mass	Nonmass	Neg	Pos	Neg	Pos	Neg	Pos	Neg	Pos
tCho (mmol/kg)	1.87	2.12	1.88	1.53	2.31	2.02	1.51	1.14	1.20	1.75	1.81	1.83	1.79	2.13	1.64
$K_{trans}$ ( $\text{min}^{-1}$ )	0.13	0.06	0.06	0.13	0.15	0.12	0.11	0.13	0.10	0.15	0.10	0.15	0.11	0.17	0.10
$k_{ep}$ ( $\text{min}^{-1}$ )	0.71	0.35	0.41	0.67	0.84	0.70	0.59	0.72	0.57	0.82	0.55	0.82	0.57	0.98	0.55

ER, estrogen receptor; HER-2, human epidermal growth factor-2; IDC, invasive ductal carcinoma; ILC, infiltrating lobular cancer; Neg, negative; Pos, positive; PR, progesterone receptor; TN, triple negative.

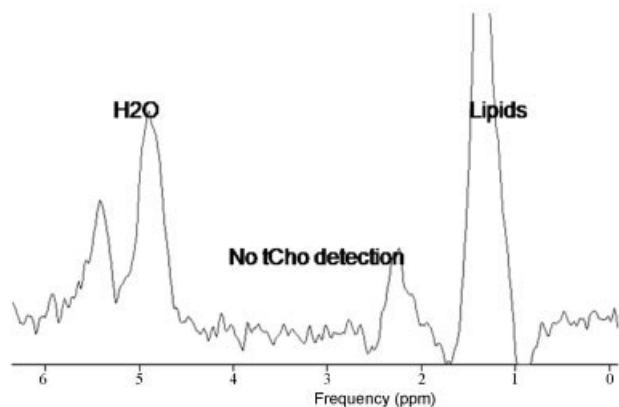
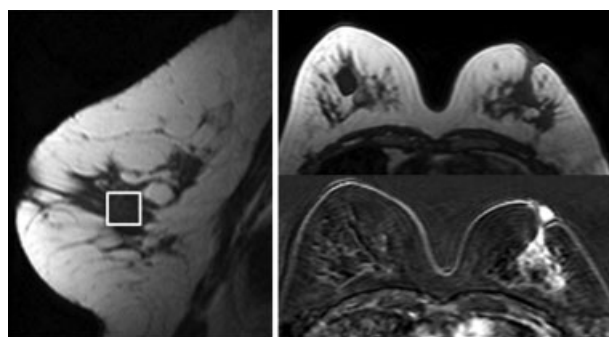


**Figure 5.** A 50-year-old woman with a  $4.1 \times 2.1$ -cm regional enhancement of infiltrative lobular cancer in the left breast. The tumor was low grade, human epidermal growth factor-2 positive and hormonal negative. The choline peak was not detectable in  $^1\text{H}$  MRS.

early relapse and reduced survival rate (32–34). HER-2-positive breast cancer is, in general, more aggressive than HER-2-negative cancer. In one study by Aboagye and Bhujwalla (35), over-expression of HER-2 in a tumor cell line resulted in a dramatic increase in choline compounds.

Younger patients were more likely to have higher choline levels ( $p = 0.05$ ). Breast cancer in young patients is known to be more aggressive and associated with a higher recurrence rate and mortality (34). In a large series of 3722 patients, Chung *et al.* (36) demonstrated that women aged less than 40 years have the poorest 5-year breast cancer-specific survival compared with all other older age groups. Tumors in young women were more likely to be at an advanced stage, high grade, ER/PR negative and lymph node positive (37). A young age is thus considered to be a poor prognostic factor and is recommended for aggressive chemotherapy, irrespective of other demographic, clinical and biological characteristics (38). The accurate diagnosis of malignant breast tumors in younger women is of particular importance for two reasons. First, the sensitivity of the mammographic examination in these patients (with denser breasts) is lower (39–41), which makes MRI/MRS a suitable adjunctive imaging modality in these women. Second, the diagnosis of benign lesions in young women is slightly higher than in the entire population, and the addition of  $^1\text{H}$  MRS may improve the diagnostic specificity. Using  $^1\text{H}$  MRS, malignant tumors in the young patient population can be diagnosed correctly with high sensitivity (100%) and specificity (89–100%) (5–7). The denser breasts in young women may yield a better spectral quality for the analysis of choline. Given all of these reasons, the inclusion of  $^1\text{H}$  MRS in the scan protocol for young women may provide very useful information.

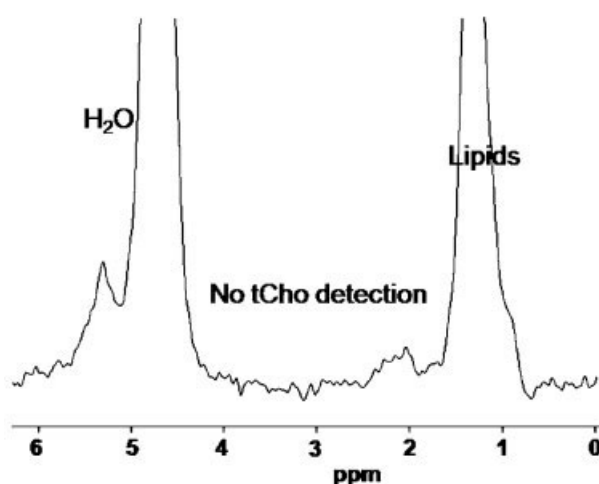
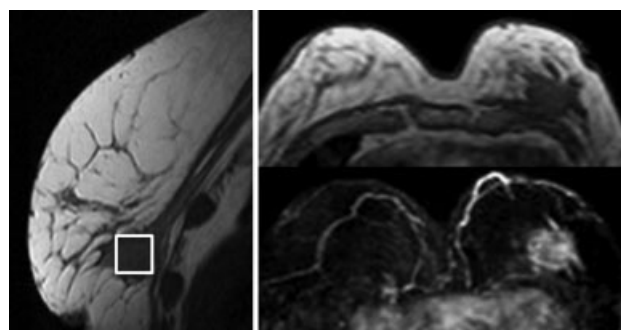


**Figure 6.** A 58-year-old woman with a  $2.8 \times 2.2$ -cm, ill-defined margin, heterogeneously enhanced, invasive ductal cancer in the left breast. The tumor was moderate grade, human epidermal growth factor-2 positive and hormonal negative. The choline peak was not detectable in  $^1\text{H}$  MRS.

It was noted that TN cancer was more likely to have high tCho than non-TN cancer ( $p = 0.09$ ). All 11 TN tumors in this study showed positive choline peaks. TN tumors, accounting for 12–26% of all types of breast cancer, are known to be more aggressive (42–47). Histologically, TN cancers are poorly differentiated, mainly of high histologic grade and have a high mitotic index (42,48).

In our study, mass lesions vs nonmass-like enhancement did not show a significant difference in tCho concentration ( $p = 0.79$ ). As nonmass-like enhancement lesions typically grow in an infiltrative pattern, measurements of their tCho level need to be taken with caution to avoid measurement contamination from the normal tissues that are intermingled with cancerous tissues within the MRS voxel. In a study by Bartella *et al.* (49),  $^1\text{H}$  MRS increased significantly the positive predictive value of biopsy for MRI-detected lesions with nonmass-like enhancement from 20% to 63%, and obviated the need for biopsy in 68% of lesions. In this study, all 12 nonmass-like enhancement cancers showed positive choline. From the illustrated cases, most presented as focal nonmass-like lesions rather than diffusely infiltrative lesions. This might be the reason why the results of Bartella *et al.* showed 100% sensitivity. In our study, cases of diffuse nonmass-like enhancement lesions were included, which may account for the lower choline detection rate.

IDC and ILC did not show a significantly different tCho level ( $p = 0.84$ ) in our study.  $^1\text{H}$  MRS has been found to be equally sensitive in other types of invasive carcinoma as well as the more common IDC (50). DCIS and IDC with an extensive *in situ*

component, however, are likely to be negative for choline at  $^1\text{H}$  MRS (51). Conversely, it is known that some fibroadenomas may present high levels of tCho *in vitro* (52) and *in vivo* (4,5,11), which may be related to their high activity of cell proliferation.

As, in this study, MRS was performed after injection of gadolinium contrast, the effect of gadolinium on the measured spectra was a concern. Bolan *et al.* (53) reported that the post-contrast tCho peak was 10% lower than the pre-contrast value, and Joe *et al.* (54) found that gadolinium increased the linewidth ( $\sim 17\%$ ) and decreased the area ( $\sim 15\%$ ) of the tCho peak. More recently, Lenkinski *et al.* (55) have reported that only the three negatively charged chelates, Magnevist, Multihance and Dotarem, broaden the choline peak in phantoms and reduce the area of the tCho peak *in vivo* by an average of about 40%. Therefore, these studies demonstrate that contrast agents can affect MRS measurements. However, it is not yet clear whether the effects of contrast agents would significantly bias MRS measurements.

The small number of subjects and the exclusion of tumors smaller than 1.5 cm were limitations of this study. With the  $^1\text{H}$  MRS voxel size of 1.5–2.0 cm, it was still possible that adjacent normal breast tissues could be included in the  $^1\text{H}$  MRS voxel, leading to a partial volume effect and reduced choline concentration.

## CONCLUSION

In this study, we have shown that higher tCho concentration is correlated significantly with higher tumor grade and higher  $K_{\text{trans}}$  and  $k_{\text{ep}}$  (greater angiogenesis). Women of younger age also tended to have a higher choline level, which is expected as younger patients are likely to have more aggressive tumors; in addition, their denser breasts may yield a better spectral quality for the analysis of choline. The results presented here may provide further understanding about the role of  $^1\text{H}$  MRS in the characterization of different breast lesions, and may aid in the better interpretation of  $^1\text{H}$  MRS for the diagnosis of breast lesions.

## Acknowledgements

This work was supported in part by the National Institutes of Health/National Cancer Institute (NIH/NCI) R01 CA127927, R01 CA90437, R03 CA136071, and by the California Breast Cancer Research Program (BCRP) #9WB-0020, 12FB-0031 and 14GB-0148.

## REFERENCES

- Ramirez de Molina A, Banez-Coronel M, Gutierrez R, Rodríguez-González A, Olmeda D, Megías D, Lacal JC. Choline kinase activation is a critical requirement for the proliferation of primary human mammary epithelial cells and breast tumor progression. *Cancer Res.* 2004; 64: 6732–6739.
- Bolan PJ, Nelson MT, Yee D, Garwood M. Imaging in breast cancer: magnetic resonance spectroscopy. *Breast Cancer Res.* 2005; 7: 149–152.
- Sitter B, Lundgren S, Bathen TF, Halgunset J, Fjøsne HE, Gribbestad IS. Comparison of HR MAS MR spectroscopic profiles of breast cancer tissue with clinical parameters. *NMR Biomed.* 2006; 19(1): 30–40.
- Kvistad KA, Bakken IJ, Gribbestad IS, Ehrnholm B, Lundgren S, Fjøsne HE, Haraldseth O. Characterization of neoplastic and normal human breast tissues with *in vivo* (1)H MR spectroscopy. *J. Magn. Reson. Imaging.* 1999; 10: 159–164.

- Yeung DK, Cheung HS, Tse GM. Human breast lesions: characterization with contrast enhanced *in vivo* proton MR spectroscopy – initial results. *Radiology.* 2001; 220: 40–46.
- Cecil KM, Schnall MD, Siegelman ES, Lenkinski RE. The evaluation of human breast lesions with magnetic resonance imaging and proton magnetic resonance spectroscopy. *Breast Cancer Res. Treat.* 2001; 68: 45–54.
- Roebuck JR, Cecil KM, Schnall MD, Lenkinski RE. Human breast lesions: characterization with proton MR spectroscopy. *Radiology.* 1998; 209: 269–275.
- Jagannathan NR, Kumar M, Seenu V, Coshic O, Dwivedi SN, Julka PK, Srivastava A, Rath GK. Evaluation of total choline from *in-vivo* volume localized proton MR spectroscopy and its response to neoadjuvant chemotherapy in locally advanced breast cancer. *Br. J. Cancer.* 2001; 84: 1016–1022.
- Tse GM, Cheung HS, Pang LM, Chu WC, Law BK, Kung FY, Yeung DK. Characterization of lesions of the breast with proton MR spectroscopy: comparison of carcinomas, benign lesions, and phyllodes tumors. *Am. J. Roentgenol.* 2003; 181: 1267–1272.
- Huang W, Fisher PR, Dulaimy K, Tudorica LA, O’Hea B, Button TM. Detection of breast malignancy: diagnostic MR protocol for improved specificity. *Radiology.* 2004; 232: 585–591.
- Bartella L, Morris EA, Dershow DD, Liberman L, Thakur SB, Moskowitz C, Guido J, Huang W. Proton MR spectroscopy with choline peak as malignancy marker improves positive predictive value for breast cancer diagnosis: preliminary study. *Radiology.* 2006; 239: 686–692.
- Katz-Brull R, Lavin PT, Lenkinski RE. Clinical utility of proton magnetic resonance spectroscopy in characterizing breast lesions. *J. Natl. Cancer Inst.* 2002; 94: 1197–1203.
- Gribbestad IS, Singstad TE, Nilsen G, Fjøsne HE, Engan T, Haugen OA, Rinck PA. *In vivo* (1)H MRS of normal breast and breast tumors using a dedicated double breast coil. *J. Magn. Reson. Imaging.* 1998; 8: 1191–1197.
- Leach MO, Verrill M, Glaholm J, Smith TA, Collins DJ, Payne GS, Sharp JC, Ronen SM, McCready VR, Powles TJ, Smith IE. Measurements of human breast cancer using magnetic resonance spectroscopy: a review of clinical measurements and a report of localized  $^{31}\text{P}$  measurements of response to treatment. *NMR Biomed.* 1998; 11: 314–340.
- Smith TA, Bush C, Jameson C, Titley JC, Leach MO, Wilman DE, McCready VR. Phospholipid metabolites, prognosis and proliferation in human breast carcinoma. *NMR Biomed.* 1993; 6: 318–323.
- Agrawal G, Chen JH, Baik HM, Hsiang D, Mehta RS, Nalcioglu O, Su MY. MR imaging features of breast cancer: a correlation study with HER-2 receptor. *Ann. Oncol.* 2007; 18(11): 1903–1904.
- Chen JH, Baik HM, Nalcioglu O, Su MY. Estrogen receptor and breast MR imaging features: a correlation study. *J. Magn. Reson. Imaging.* 2008; 27(4): 825–833.
- Baik HM, Chen JH, Nalcioglu O, Su MY. Choline as a biomarker for cell proliferation: do the results from proton MR spectroscopy show difference between HER2/neu positive and negative breast cancers? *Int. J. Cancer.* 2008; 123(5): 1219–1221.
- Bottomley PA. Spatial localization in NMR spectroscopy *in vivo*. *Ann. NY Acad. Sci.* 1987; 508: 333–348.
- Hasse A, Frahm J, Hanicke W, Matthaei D.  $^1\text{H}$  NMR chemical shift selective (CHESS) imaging. *Phys. Med. Biol.* 1985; 30: 341–344.
- Bolan PJ, Meisamy S, Baker EH, Lin J, Emory T, Nelson M, Everson LI, Yee D, Garwood M. *In vivo* quantification of choline compounds in the breast with  $^1\text{H}$  MR spectroscopy. *Magn. Reson. Med.* 2003; 50: 1134–1143.
- Baik HM, Su MY, Yu H, Mehta R, Nalcioglu O. Quantification of choline-containing compounds in malignant breast tumors by  $^1\text{H}$  MR spectroscopy using water as an internal reference at 1.5 T. *MAGMA.* 2006; 19: 96–104.
- Tofts PS. Modeling tracer kinetics in dynamic Gd-DTPA MR imaging. *J. Magn. Reson. Imaging.* 1997; 7: 91–101.
- Tofts PS, Brix G, Buckley D, Evelhoch JL, Henderson E, Knopp MV, Larsson HB, Lee TY, Mayr NA, Parker GJ, Port RE, Taylor J, Weisskoff RM. Estimating kinetics parameters from dynamic contrast-enhanced T1-weighted MRI of a diffusible tracer: standardized quantities and symbols. *J. Magn. Reson. Imaging.* 1999; 10: 223–232.
- American College of Radiology. *Breast Imaging Reporting and Data System Atlas (BI-RADS atlas)*. American College of Radiology: Reston, VA, 2003.



26. Stanwell P, Gluch L, Clark D, Tomanek B, Baker L, Giuffrè B, Lean C, Malycha P, Mountford C. Specificity of choline metabolites for in vivo diagnosis of breast cancer using <sup>1</sup>H MRS at 1.5 T. *Eur. Radiol.* 2005; 15: 1037–1043.
27. Su MY, Baik HM, Yu HJ, Chen JH, Mehta RS, Nalcioglu O. Comparison of choline and pharmacokinetic parameters in breast cancer measured by MR spectroscopic imaging and dynamic contrast enhanced MRI. *Technol. Cancer Res. Treat.* 2006; 5: 401–410.
28. Baik HM, Yu HJ, Chen JH, Nalcioglu O, Su MY. Quantitative correlation between (1)H MRS and dynamic contrast-enhanced MRI of human breast cancer. *Magn. Reson. Imaging.* 2008; 26(4): 523–531.
29. Ramirez de Molina A, Gutierrez R, Ramos MA, Silva JM, Silva J, Bonilla F, Sánchez JJ, Lacal JC. Increased choline kinase activity in human breast carcinomas: clinical evidence for a potential novel antitumor strategy. *Oncogene.* 2002; 21: 4317–4322.
30. Yarden Y. Biology of HER2 and its importance in breast cancer. *Oncology.* 2001; 61(Suppl 2): 1–13.
31. Holbro T, Civenni G, Hynes NE. The ErbB receptors and their role in cancer progression. *Exp. Cell Res.* 2003; 284: 99–110.
32. Nahta R, Esteva FJ. Herceptin: mechanisms of action and resistance. *Cancer Lett.* 2006; 232: 123–138.
33. Stefano R, Agostara B, Calabro M, Campisi I, Ravazzolo B, Traina A, Miele M, Castagnetta L. Expression levels and clinical–pathological correlations of HER2/neu in primary and metastatic human breast cancer. *Ann. NY Acad. Sci.* 2004; 1028: 463–472.
34. Tokatli F, Altaner S, Uzal C, Ture M, Kocak Z, Uygun K, Bilgi S. Association of HER-2/neu overexpression with the number of involved axillary lymph nodes in hormone receptor positive breast cancer patients. *Exp. Oncol.* 2005; 27: 145–149.
35. Aboagye EO, Bhujwala ZM. Malignant transformation alters membrane choline phospholipid metabolism of human mammary epithelial cells. *Cancer Res.* 1999; 59: 80–84.
36. Chung M, Chang HR, Bland KI, Wanebo HJ. Younger women with breast carcinoma have a poorer prognosis than older women. *Cancer.* 1996; 77: 97–103.
37. Bharat A, Aft RL, Gao F, Margenthaler JA. Patient and tumor characteristics associated with increased mortality in young women (<math>\leq 40</math> years) with breast cancer. *J. Surg. Oncol.* 2009; 100(3): 248–251.
38. Thuerlimann B. International consensus meeting on the treatment of primary breast cancer 2001, St. Gallen, Switzerland. *Breast Cancer.* 2001; 8: 294–297.
39. Kerlikowske K, Grady D, Barclay J, Sickles EA, Ernster V. Effect of age, breast density, and family history on the sensitivity of first screening mammography. *J. Am. Med. Assoc.* 1996; 276: 33–38.
40. Johnstone PA, Moore EM, Carrillo R, Goepfert CJ. Yield of mammography in selected patients age  $\leq 30$  years. *Cancer.* 2001; 91: 1075–1078.
41. Wang J, Shih TT, Hsu JC, Li YW. The evaluation of false negative mammography from malignant and benign breast lesions. *Clin. Imaging.* 2000; 24: 96–103.
42. Haffty BG, Yang Q, Reiss M, Kearney T, Higgins SA, Weidhaas J, Harris L, Hait W, Toppmeyer D. Loco-regional relapse and distant metastasis in conservatively managed triple negative early-stage breast cancer. *J. Clin. Oncol.* 2006; 24(36): 5652–5657.
43. Rakha EA, El-Sayed ME, Green AR, Lee AH, Robertson JF, Ellis IO. Prognostic markers in triple-negative breast cancer. *Cancer.* 2007; 109(1): 25–32.
44. Cleator S, Heller W, Coombes RC. Triple-negative breast cancer: therapeutic options. *Lancet Oncol.* 2007; 8(3): 235–244.
45. Carey LA, Perou CM, Livasy CA, Dressler LG, Cowan D, Conway K, Karaca G, Troester MA, Tse CK, Edmiston S, Deming SL, Geradts J, Cheang MC, Nielsen TO, Moorman PG, Earp HS, Millikan RC. Race, breast cancer subtypes, and survival in the Carolina Breast Cancer Study. *J. Am. Med. Assoc.* 2006; 295: 2492–2502.
46. Bauer KR, Brown M, Cress RD, Parise CA, Caggiano V. Descriptive analysis of estrogen receptor (ER)-negative, progesterone receptor (PR)-negative, and HER2-negative invasive breast cancer, the so-called triple-negative phenotype: a population-based study from the California Cancer Registry. *Cancer.* 2007; 109(9): 1721–1728.
47. Glunde K, Ackerstaff E, Mori N, Jacobs MA, Bhujwala ZM. Choline phospholipid metabolism in cancer: consequences for molecular pharmaceutical interventions. *Mol. Pharm.* 2006; 3: 496–506.
48. Siziopikou KP, Cobleigh M. The basal subtype of breast carcinomas may represent the group of breast tumors that could benefit from EGFR-targeted therapies. *Breast.* 2007; 16(1): 104–107.
49. Bartella L, Thakur SB, Morris EA, Dershaw DG, Huang W, Chough E, Cruz MC, Liberman L. Enhancing nonmass lesions in the breast: evaluation with proton (<sup>1</sup>H) MR spectroscopy. *Radiology.* 2007; 245(1): 80–87.
50. Tse GM, Yeung DK, King AD, Cheung HS, Yang WT. In vivo proton magnetic resonance spectroscopy of breast lesions: an update. *Breast Cancer Res. Treat.* 2007; 104(3): 249–255.
51. Yeung DK, Yang WT, Tse GM. Breast cancer: in vivo proton MR spectroscopy in the characterization of histopathologic subtypes and preliminary observations in axillary node metastases. *Radiology.* 2002; 225(1): 190–197.
52. Mackinnon WB, Barry PA, Malycha PL, Gillett DJ, Russell P, Lean CL, Doran ST, Barraclough BH, Bilous M, Mountford C. Fine-needle biopsy specimens of benign breast lesions distinguished from invasive cancer ex vivo with proton MR spectroscopy. *Radiology.* 1997; 204: 661–666.
53. Bolan PJ, Baker E, DelaBarre L, Merkle H, Yee D, Everson LI, Garwood M. Effects of Gd-DTPA on breast <sup>1</sup>H MRS at 4T. *Proceedings of the 87th Annual Meeting of the Radiological Society of North America*, Chicago, IL, USA, 2001.
54. Joe BN, Chen VY, Salibi N, Fuangtharntip P, Hildebolt CF, Bae KT. Evaluation of <sup>1</sup>H-magnetic resonance spectroscopy of breast cancer pre- and postgadolinium administration. *Invest. Radiol.* 2005; 40: 405–411.
55. Lenkinski RE, Wang X, Elian M, Goldberg SN. Interaction of gadolinium-based MR contrast agents with choline: implications for MR spectroscopy (MRS) of the breast. *Magn. Reson. Med.* 2009; 61(6): 1286–1292.